

# Durable Silicon Rubber-Based Miniaturized Antenna with Concentric Circle Structure for Medical Telemetry Application

Navin M. George\* and Thomas Anita Jones Mary Pushpa

**Abstract**—In this paper, a low-profile flexible antenna using a flexible substrate is presented. The proposed antenna has concentric circle-shaped radiating elements with circular slots to achieve an ISM band. The flexible antenna having dimensions (33 mm × 18 mm × 2 mm) is designed and fabricated on a silicon rubber-based substrate, and measurements were performed to validate the simulation results. The measured and simulated results demonstrate that the antenna radiates at 2.45 GHz center frequency, with a return loss of  $-23.23$ . The operating frequency of 2.45 GHz, flexible substrate, and low SAR of 0.0658 W/kg confirm that the proposed antenna is suitable for medical telemetry applications.

## 1. INTRODUCTION

Flexible antennas are considered the future in medical telemetry applications, and research is going on to optimize antenna performances. There are challenges in achieving the parameters of a flexible antenna within permissible limits. Different structures are etched in the radiating part and ground plane to tune the antenna to the desired operating frequency band. A series of six rectangular slots are introduced in the ground plane [1] to have an excellent current distribution in the inset-fed microstrip radiating patch. The reflection coefficient characteristics are improved by having the defected ground structure (DGS) [1]. The antenna for biomedical applications [2] has a U-shaped microstrip patch antenna with meandered slots embedded on it, and the antenna is tuned at 2.45 GHz resonant frequency. A specific absorption rate (SAR) analysis has been carried out for the rectangular loop shape antenna for biomedical applications [3] at a particular resonant frequency. The literary works [1–3] SAR analysis is not mentioned in the article.

An  $\Omega$ -shaped metamaterial structure design is integrated with the ground plane [4] to enhance the gain of the wearable antenna. The arc-shaped conductive sheet [5] in a polydimethylsiloxane (PDMS) based flexible substrate shows that the SAR is reduced for the operating frequency range by using a complete ground plane in the design. A partial ground plane is used with radiating patches having rectangular slots [6] to enhance the operating bandwidth. The radiating patches with a parasitic element and defected ground structure (DGS) with hexagonal slots [7] are designed to operate at 2.45 GHz in on-body communication.

The antenna operates in different resonant frequencies [10–13] using a radiating strip structure. The radiating strip length considered in the literary works is between monopole and dipole design length. To have a compact design, circular shape radiating structures are proposed in the literature [14–19]. The wearable devices should be compact and flexible to integrate with wearable applications. A concentric circular shape radiating patch with a circular slot embedded on it is with a partial ground plane which is presented in the proposed antenna design.

---

*Received 25 October 2021, Accepted 17 January 2022, Scheduled 19 January 2022*

\* Corresponding author: Navin M. George (mnavingeorge@gmail.com).

The authors are with the Department of Electronics and Communication, Karunya Institute of Technology and Sciences, Coimbatore, India.

## 2. ANTENNA DESIGN

The trimetric structure of the proposed antenna for medical telemetry application is depicted in Figure 1. A long microstrip feedline with a thick stub is implemented in the proposed design. Concentric circles are designed on the top of a silicon substrate to improve antenna characteristics and achieve miniaturization. The concentric rings are responsible for achieving the center frequency of 2.45 GHz at the ISM band. A partial ground plane is implemented in the proposed antenna since it reduces the energy stored in the substrate and improves the bandwidth.

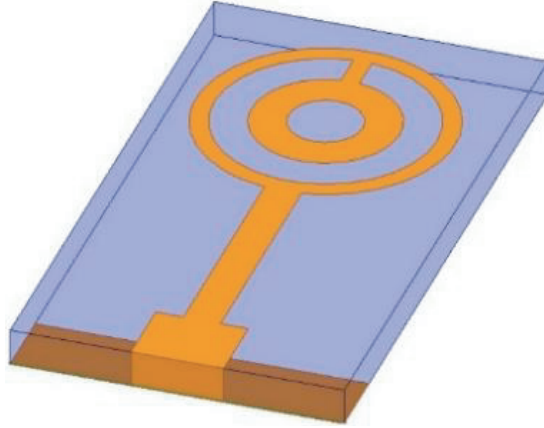


**Figure 1.** Trimetric view of the designed antenna.

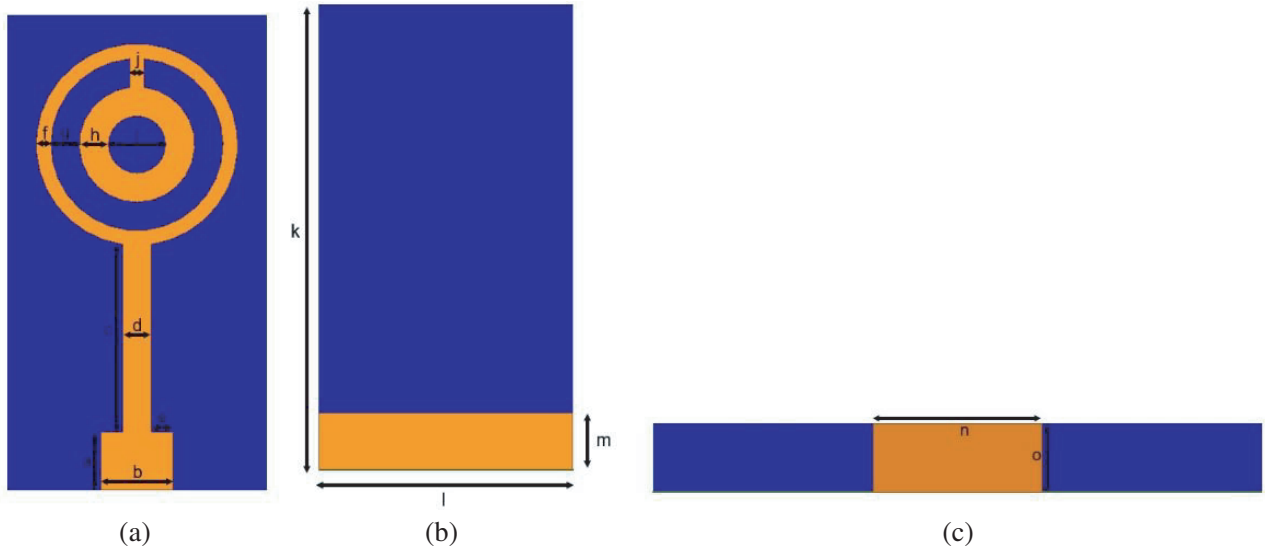


**Figure 2.** Antenna geometry: (a) Top view; (b) Bottom view; (c) Side view (feed).

The antenna geometry of the proposed antenna is exhibited in Figure 2. The surface area of the durable silicon substrate is 33 mm × 18 mm. The relative permittivity of the substrate is  $\epsilon_r = 2.93$ , with a thickness of 2 mm. Table 1 demonstrates the geometry of the proposed structure.

The resonant frequency for the concentric ring structure is theoretically calculated as follows [19], and the equations below will derive the resonant frequency 2.45 GHz, respectively.

$$f_{ring} = \frac{Ac}{2\pi R\sqrt{\epsilon_{re}}} \quad (1)$$

**Table 1.** Dimensions of the proposed antenna.

| Basic Configuration | Parameters | Value (mm) |
|---------------------|------------|------------|
| Radiating Element   | <i>a</i>   | 4          |
|                     | <i>b</i>   | 5          |
|                     | <i>c</i>   | 16         |
|                     | <i>d</i>   | 2          |
|                     | <i>e</i>   | 1.5        |
|                     | <i>f</i>   | 1          |
|                     | <i>g</i>   | 2          |
|                     | <i>h</i>   | 2          |
|                     | <i>i</i>   | 4          |
|                     | <i>j</i>   | 1          |
| Ground Plane        | <i>k</i>   | 33         |
|                     | <i>l</i>   | 18         |
|                     | <i>m</i>   | 4          |
| Feeding             | <i>n</i>   | 5          |
|                     | <i>o</i>   | 2          |

$$A = \frac{2R}{(R + T) + R} \tag{2}$$

$$\epsilon_{re} = \frac{1}{2}(\epsilon_r, sub + 1) + \frac{1}{2}(\epsilon_r, sub - 1) \left(1 + \frac{10H_s}{T}\right)^{-\frac{1}{2}} \tag{3}$$

where  $\epsilon_{re}$  is the effective relative permittivity, and  $\epsilon_r$  is the substrate permittivity.  $H_s$  is the height of the substrate, and  $R, T$  are the radius and thickness of the concentric ring, respectively.

### 3. PARAMETRIC ANALYSIS

#### 3.1. Impact of Center Slot

A parametric analysis study has been conducted based on the difference in structure, as shown in Figure 3. The design has been classified as without a circular center slot in Figure 3(a) and with a

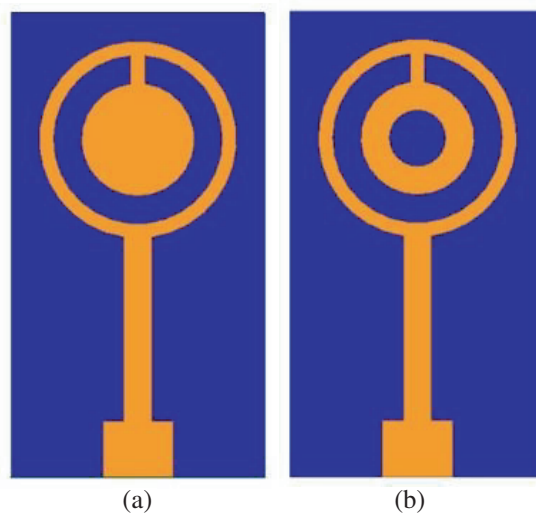


**Figure 3.** Proposed antenna with and without circular center slot: (a) Without circular center slot; (b) With the circular center slot.

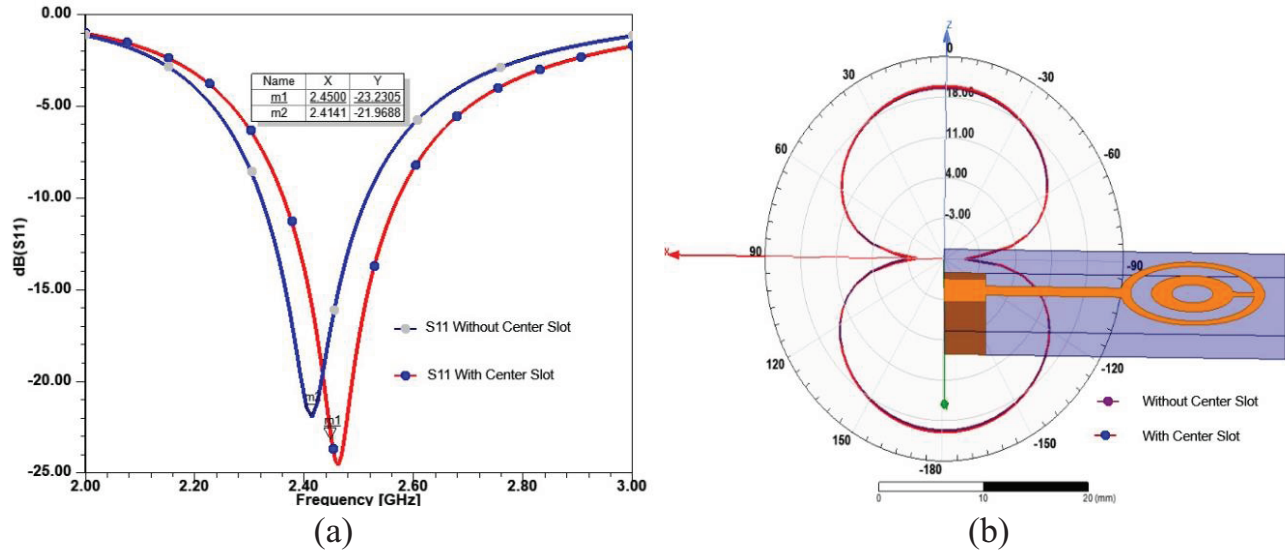


**Figure 4.** Simulated results of the proposed antenna with and without center slot: (a)  $S_{11}$ , (b) 2D radiation pattern in (XZ) plane.

circular center slot in Figure 3(b). A circular slot of 4 mm diameter is made in the second iteration, giving a better response in terms of antenna parameters in Figure 4.

The parametric study states that the ( $S_{11}$ ) return loss parameter (see Figure 4(a)) of the design without a circular slot gives  $-21.96$  dB at 2.41 GHz. The design with a circular slot gives a better return loss of  $-23.23$  dB at 2.45 GHz. The radiation pattern parameter (see Figure 4(b)) of the design without a circular slot gives 19.94 dB, and the design with a circular slot gives 19.93 dB. The design with a circular slot at the center performs better from the above results.

### 3.2. Impact of Bending

A bending analysis is an inevitable factor to analyze the performance of a flexible antenna. The proposed antenna is simulated with a bending angle of  $37.77^\circ$  in Figure 5. The ( $S_{11}$ ) return loss parameter (see Figure 6(a)) of the antenna under bending condition gives  $-21.96$  dB at 2.41 GHz, and the design

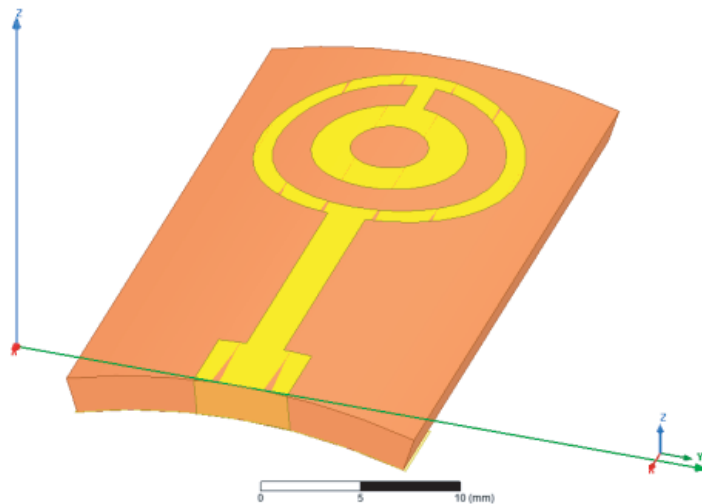


**Figure 5.** Proposed antenna under bending conditions.

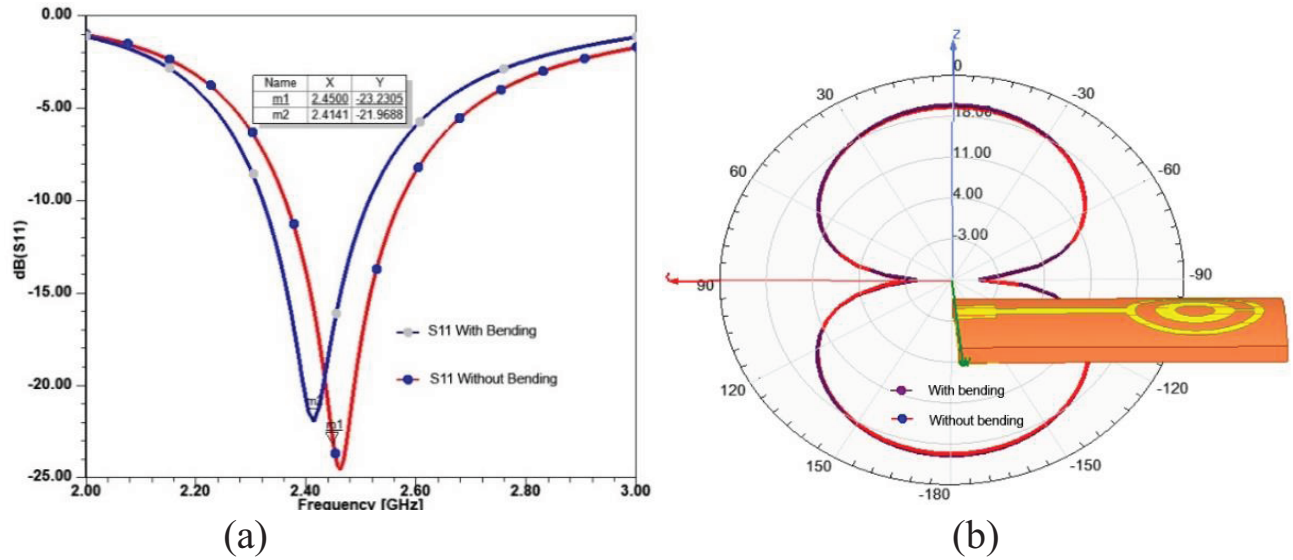


**Figure 6.** Simulated results of the proposed antenna with and without bending conditions: (a)  $S_{11}$ , (b) 2D radiation pattern in ( $XZ$ ) plane.

without bending gets  $-23.23$  dB at 2.45 GHz.

Concerning the radiation pattern parameter, Figure 6(b) of the antenna under bending condition shows 19.60 dBi, and the design without bending gives 19.93 dBi. The performance of the design under bending conditions does not have many variations from that under non-bending-conditions. Hence, the proposed antenna is very well adapted to bending conditions and can be used for flexible applications.

The gain of the proposed antenna is 2.17 dBi under non-bending condition and 1.91 dBi under bending condition (see Figure 7(a)), and the radiation efficiency is obtained as 92.61% in non-bending condition and 90.19% under bending condition (see Figure 7(b)). From the radiation efficiency and return loss, the total efficiency obtained under non bending condition is 90.33% and under bending is 89.61%.

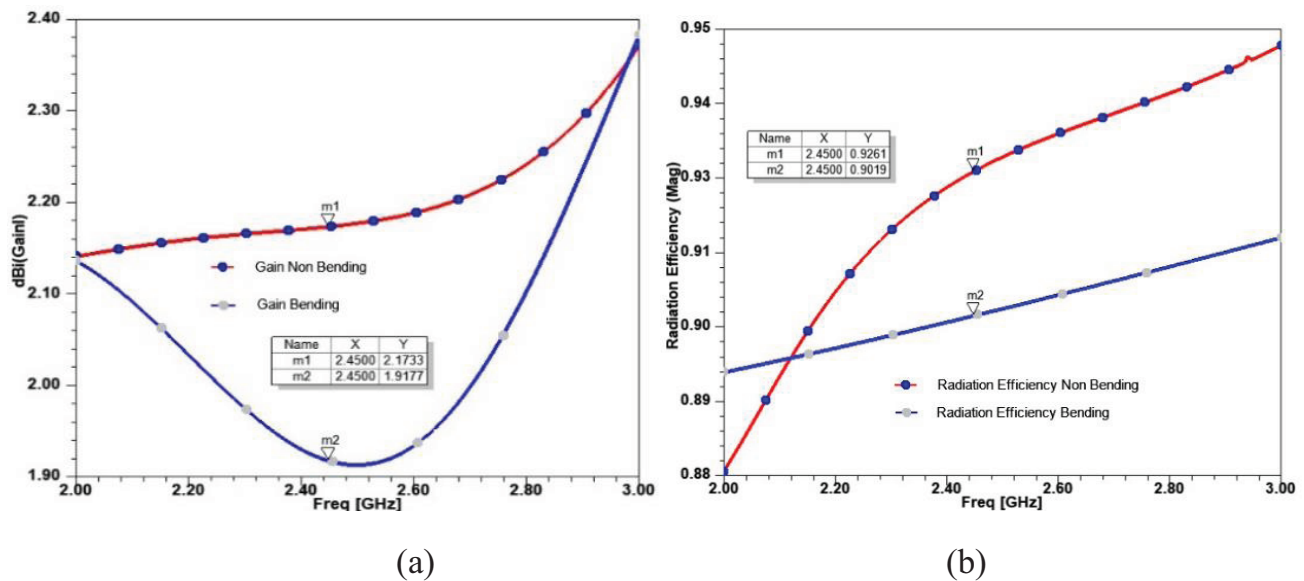


**Figure 7.** Other parameters of the proposed antenna: (a) Gain of the proposed antenna; (b) Radiation efficiency of the proposed antenna.

## 4. MEASURED RESULTS AND DISCUSSIONS

### 4.1. Simulated and Measured under Non-Bending Conditions

The proposed antenna is fabricated using a silicon-based rubber substrate of thickness 2 mm with a copper conductor thickness of 0.04 mm. The design is exported from HFSS as CAD, and the conducting material was cut using a CNC wire cut EDM machine. The cut material was glued onto the substrate and connected to an SMA connector using a coaxial cable. The fabricated antenna is tested using a Keysight field fox network analyzer. The fabricated antenna's top view and bottom view are shown in Figure 8.

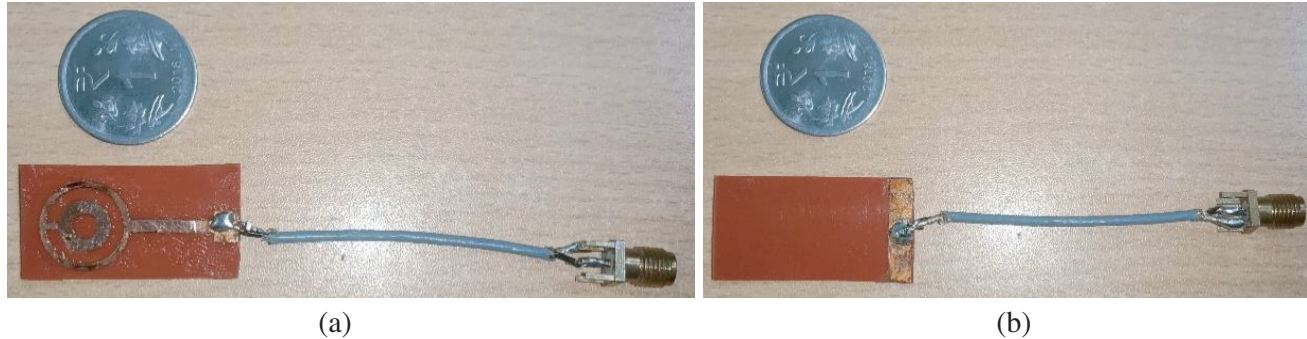


**Figure 8.** Fabricated antenna using silicon substrate: (a) Top view; (b) Bottom view.

When testing is performed for the prototype under non-bending conditions, the ( $S_{11}$ ) return loss parameter (see Figure 9(a)) of the antenna under simulation is  $-23.23$  dB at 2.45 GHz. Under testing antenna gives  $-16.10$  dB at 2.45 GHz. Concerning Voltage Standing Wave Ratio (VSWR) parameter, Figure 9(b) shows that the VSWR of the antenna is 1.33 at 2.45 GHz and 1.20 at 2.45 GHz under testing. Concerning the impedance parameter, Figure 9(c) shows that the antenna impedance is 58.28 at 2.45 GHz under simulation and 53.57 at 2.45 GHz under testing. The 3D radiation pattern of the antenna is shown in Figure 9(d). The performance of the proposed design under test does not deviate much from the simulated results under non-bending conditions. Hence, it can be concluded that the proposed antenna behaves well in real-time situations and is very apt for flexible applications.

### 4.2. Simulated and Measured under Bending Conditions

When testing is performed for the prototype under bending conditions (see Figure 10), the ( $S_{11}$ ) return loss parameter (see Figure 11(a)) of the antenna under simulation is  $-21.96$  dB at 2.41 GHz. Under testing it gives  $-40.13$  dB at 2.48 GHz. Concerning Voltage Standing Wave Ratio (VSWR) parameter, Figure 11(b) shows that the VSWR of the antenna under simulation is 1.37 at 2.45 GHz and 1.40 at 2.51 GHz under testing. Concerning the Impedance parameter, Figure 11(c) shows that the antenna impedance is 50.76 at 2.42 GHz under simulation and 48.32 at 2.43 GHz under testing. The 3D radiation pattern of the antenna is shown in Figure 11(d). The performance of the proposed design under test does not deviate much from the simulated results under bending conditions. With this, the proposed antenna is said to behave well in real-time testing under bending conditions and can be very much utilized for flexible applications.

## 5. SAR ANALYSIS

### 5.1. Using Heterogeneous Phantom

(SAR) is analyzed using a four-layer heterogeneous phantom (see Figure 12(a)) for the proposed antenna design. The skin layer has a permittivity of 18.99, conductivity of 22.841, and thickness of 2 mm. The fat layer has a permittivity of 3.86, conductivity of 1.48, and thickness of 5 mm. The muscle layer has a

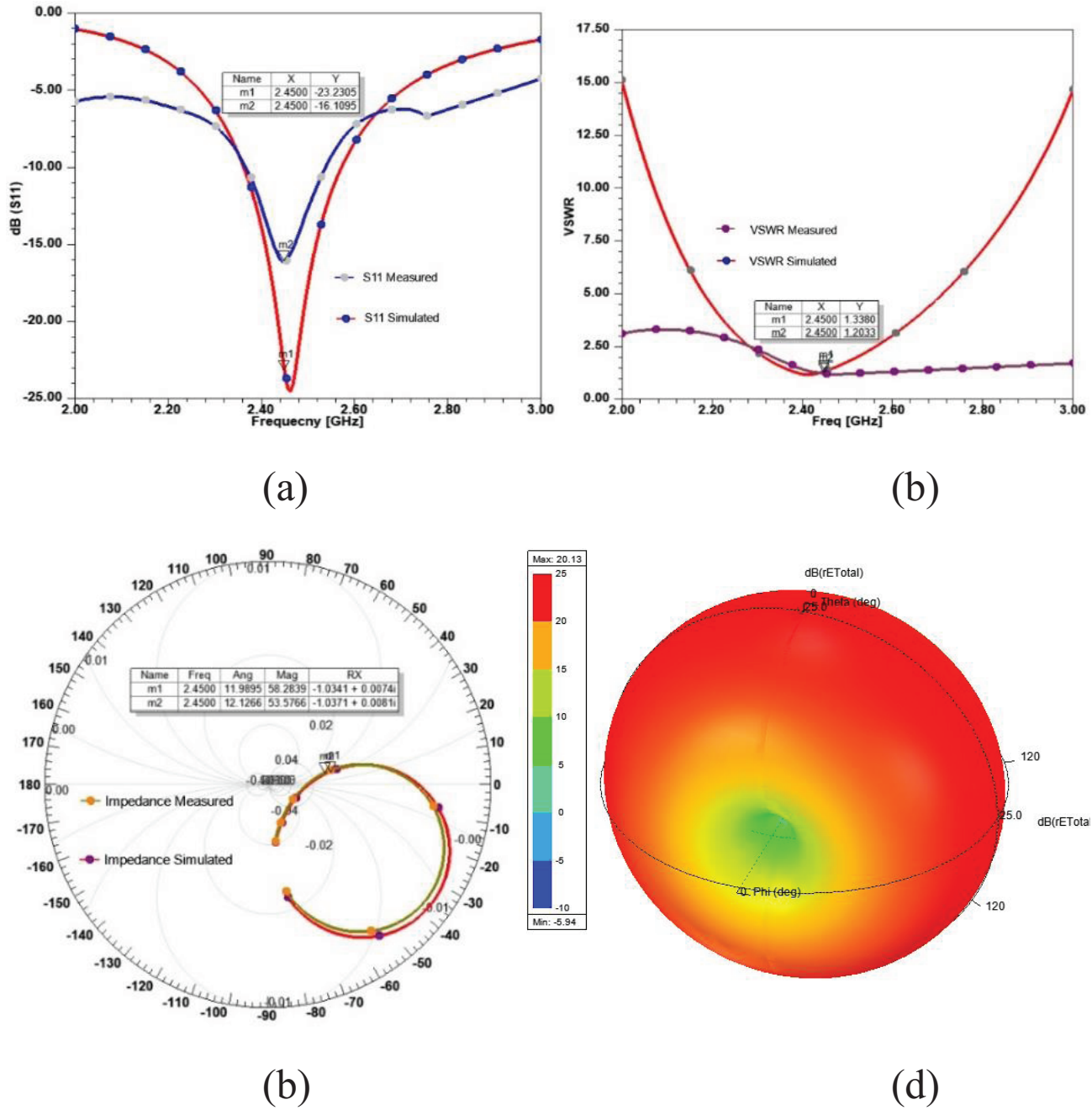


**Figure 9.** Simulated and measured results: (a)  $S_{11}$  return loss; (b) VSWR; (c) Impedance; (d) 3D radiation pattern (simulated).

permittivity of 27.39, conductivity of 29.437, and thickness of 10 mm. The bone layer has a permittivity of 8.17, conductivity of 8.0309, and thickness of 10 mm. The proposed design is kept 2 mm away from the phantom model for SAR analysis. The input power given to the antenna for analysis is 1 Watt. The total radiated power from the antenna is 922.12 mW. This analysis is done for the on-body antenna to ensure that the antenna is safe for body application.

$$SAR = \frac{\sigma \times E^2}{m_d} \tag{4}$$

$\sigma = \text{conductivity of material}$

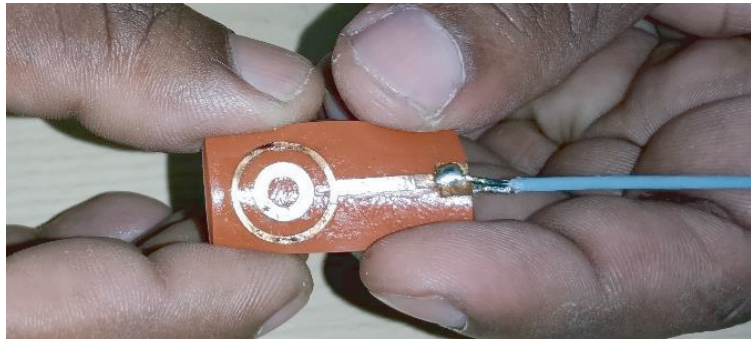


Figure 10. Fabricated antenna measured under bending conditions.

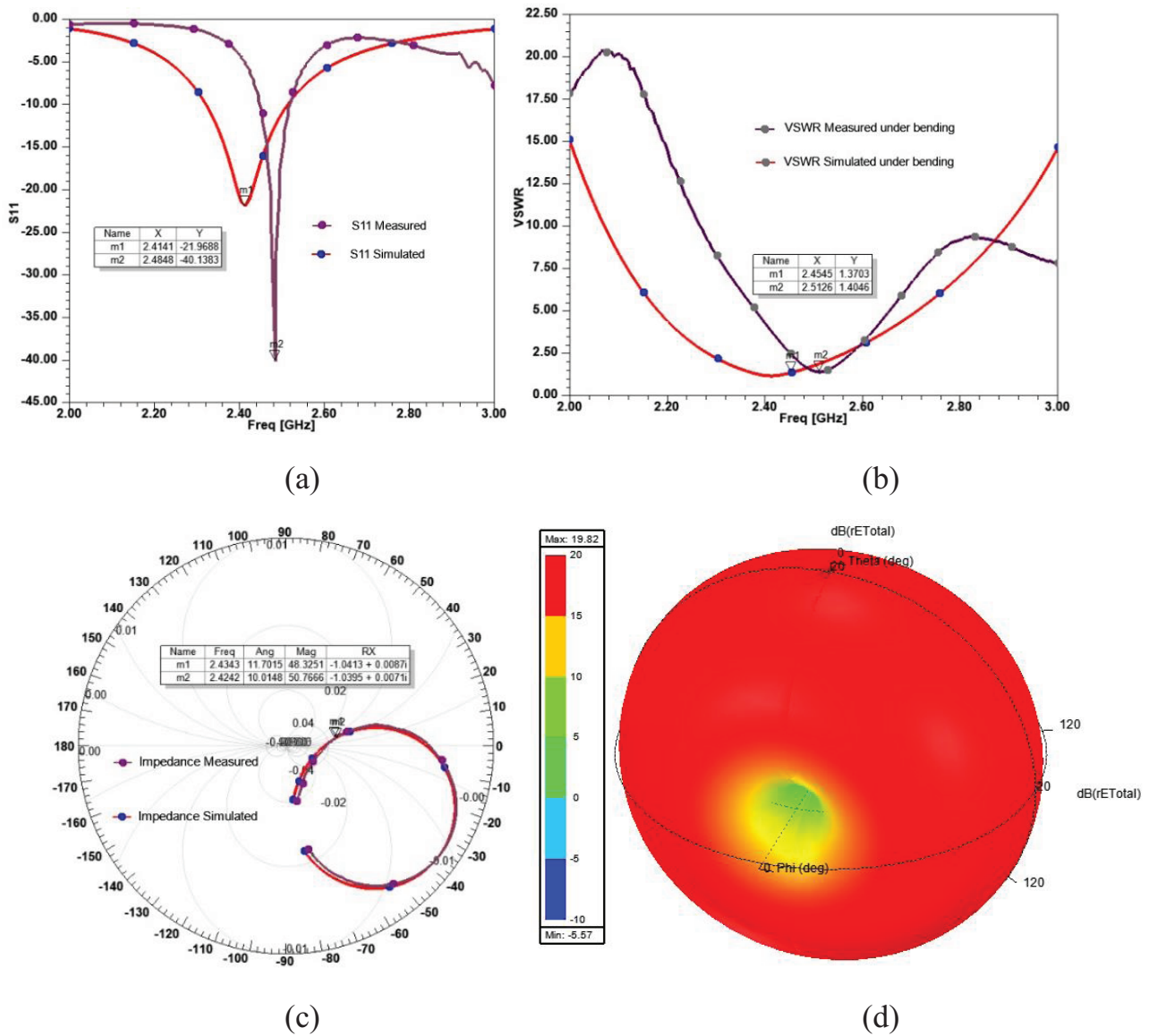
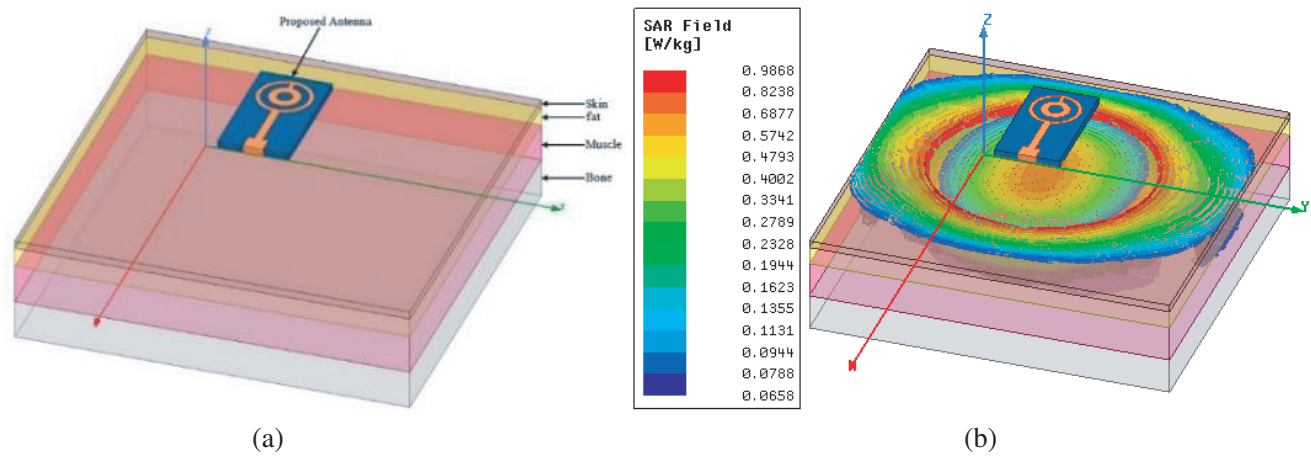


Figure 11. Simulated and measured results with bending: (a)  $S_{11}$  return loss; (b) VSWR; (c) Impedance; (d) 3D radiation pattern (simulated).



$$E = \text{electric field}$$

$$m_d = \text{mass density}$$



**Figure 12.** SAR analysis: (a) Proposed antenna in the heterogeneous phantom model; (b) SAR field distribution of the proposed antenna.

The specific absorption rate of the proposed antenna design simulated with heterogeneous phantom shows a maximum of 0.9868 W/kg and minimum of 0.0658 W/kg, as shown in Figure 12(b). The proposed antenna design offers a SAR value less than the permissible limits. Hence, the proposed antenna can be used for on-body communications.

**Table 2.** Comparison of the proposed antenna with existing ones.

| Year, Ref. | Antenna Size (mm <sup>2</sup> ) | Substrate               | Flexible/ Not-Flexible | Resonant Frequency (GHz) | Gain (dBi) | Efficiency (%) | SAR   |
|------------|---------------------------------|-------------------------|------------------------|--------------------------|------------|----------------|---|
| 019, [1]   | 46 × 38                         | Taconic TLX-8           | Not Flexible           | 2.45                     | 5.65       | —              | —   |
| 2017, [2]  | 35 × 29                         | FR4                     | Not-Flexible           | 2.45                     | -20        | —              | —   |
| 2018, [3]  | 16 × 16                         | Teflon                  | Not-Flexible           | 2.45                     | -20        | —              | —   |
| 2020, [4]  | 60 × 60                         | Felt Fabric             | Flexible               | 2.45                     | 7.79 dB    | —              | 0.405 W/kg  |
| 2018, [5]  | 80 × 67                         | PDMS                    | Flexible               | 3.7–10.3                 | 4.53       | 25%            | 0.147 W/kg at 5 GHz, 0.174 W/kg at 7 GHz          |
| 2020, [6]  | 17 × 25                         | RT/duroid               | Semi-flexible          | 2.4                      | 2.5        | 93%            | < 1.6 W/kg for an input power of less than 265 mW |
| 2020, [7]  | 25 × 20                         | Kapton polyimide        | Flexible               | 2.46                     | -1.84      | —              | 1 W/kg  |
| 2020, [8]  | 50 × 50                         | Graphene-assembled film | Flexible               | 3.13–4.42 GHz            | —          | —              | —   |
| 2021, [9]  | 25 × 30                         | Jean                    | Flexible               | 3.9–11                   | 2.3–4.4    | 65–82%         | 0.88–1.02 W/kg                                    |
| Proposed   | 33 × 18                         | Silicon Rubber          | Flexible               | 2.45                     | 2.17       | 92.61%         | 0.06–0.98 W/kg                                    |

## 6. COMPARISON WITH OTHER STUDIES

According to the references in Table 2 from [1–3], all the antennas are not flexible and cannot be used for the medical on-body application, and also the size of the antenna is not small. SAR is not analyzed for the mentioned antennas. References [4–9] are all flexible substrates with a reasonable gain and permissible SAR with good efficiency. When miniaturization is considered, the proposed antenna is reduced to 87.15 percent of that of the design which has been computed out of the equations. Hence, the proposed antenna has a less area with a flexible substrate, operates in ISM band with a considerably good gain and low SAR within permissible results, and also achieves better efficiency.

## 7. CONCLUSION

A durable silicon rubber-based miniaturized antenna with a concentric circle structure is examined for medical telemetry application working at the center frequency of 2.45 GHz. The proposed antenna is simulated and tested under bending condition. SAR analysis is performed, and better performance than the existing ones depicted in Table [3] is obtained. The bending test was done for the proposed antenna and received only a minor variation with results. SAR analysis is also done for the proposed design, and a minimum SAR value within the permissible range is obtained. The proposed design has also achieved miniaturization for on-body application. Hence, the antenna is very much suitable for medical telemetry applications. Future research will be focused more on the use of metamaterials as substrate.

## REFERENCES

1. Islam, M. S., M. I. Ibrahimy, S. M. A. Motakabber, A. Z. Hossain, and S. K. Azam, "Microstrip patch antenna with defected ground structure for biomedical application," *Bulletin of Electrical Engineering and Informatics*, Vol. 8, No. 2, 586–595, 2019.
2. Sukhija, S. and R. K. Sarin, "A U-shaped meandered slot antenna for biomedical applications," *Progress In Electromagnetics Research M*, Vol. 62, 65–77, 2017.
3. Kumar, S. A., M. A. Raj, and T. Shanmuganatham, "Analysis and design of CPW fed antenna at ISM band for biomedical applications," *Alexandria Engineering Journal*, Vol. 57, No. 2, 723–727, 2018.
4. Das, G. K., S. Basu, B. Mandal, D. Mitra, R. Augustine, and M. Mitra, "Gain-enhancement technique for wearable patch antenna using grounded metamaterial," *IET Microwaves, Antennas & Propagation*, Vol. 14, No. 15, 2045–2052, 2020.
5. Simorangkir, R. B., A. Kiourti, and K. P. Esselle, "UWB wearable antenna with a full ground plane based on PDMS-embedded conductive fabric," *IEEE Antennas and Wireless Propagation Letters*, Vol. 17, No. 3, 493–496, 2018.
6. Smida, A., A. Iqbal, A. J. Alazemi, M. I. Waly, R. Ghayoula, and S. Kim, "Wideband wearable antenna for biomedical telemetry applications," *IEEE Access*, Vol. 8, 15687–15694, 2020.
7. Naik, K. K., S. C. S. Teja, B. V. Sailaja, and P. A. Sri, "Design of flexible parasitic element patch antenna for biomedical application," *Progress In Electromagnetics Research M*, Vol. 94, 143–153, 2020.
8. Zhang, J., et al., "Flexible graphene-assembled film-based antenna for wireless wearable sensor with miniaturized size and high sensitivity," *ACS Omega*, Vol. 5, No. 22, 12937–12943, American Chemical Society (ACS), May 30, 2020.
9. Kanagasabai, M., P. Sambandam, M. G. N. Alsath, S. Palaniswamy, A. Ravichandran, and C. Girinathan, "Miniaturized circularly polarized UWB antenna for body centric communication," *IEEE Transactions on Antennas and Propagation*, Vol. 7, No. 1, 189–196, 2022.
10. Vummadisetty, P. N. and A. Kumar, "Multi feed multi band uniplanar ACS fed antenna with N shape and inverted L shape radiating branches for wireless applications," *Microsystem Technologies*, Vol. 24, No. 4, 1863–1873, 2018.

11. Gunamony, S. L. and J. B. Gnanadhas, "Design and investigations of miniaturized dual-band quarter concentric circular ring antenna for LTE and 5G applications," *Arabian Journal for Science and Engineering*, 1–10, 2021.
12. Ameen, M., R. Chowdhury, and R. K. Chaudhary, "ACS-fed electrically small metamaterial inspired dual polarized antenna enabled with staircase radiating strips for UMTS/WiMAX/WLAN applications," *2019 Photonics & Electromagnetics Research Symposium — Spring (PIERS — Spring)*, 587–594, Rome, Italy, June 17–20, 2019.
13. Naidu, P. V., A. Kumar, and R. Rengasamy, "Uniplanar ACS fed multiband high-gain antenna with extended rectangular strips for portable system applications," *International Journal of RF and Microwave Computer-Aided Engineering*, Vol. 29, No. 10, e21870, 2019.
14. Dastranj, A., F. Ranjbar, and M. Bornapour, "A new compact circular shape fractal antenna for broadband wireless communication applications," *Progress In Electromagnetics Research C*, Vol. 93, 19–28, 2019.
15. Singh, V., B. Mishra, A. K. Dwivedi, and R. Singh, "Inverted L-notch loaded hexa band circular patch antenna for X, Ku/K band applications," *Microwave and Optical Technology Letters*, Vol. 60, No. 8, 2081–2088, 2018.
16. Ujwal Prakash, A. J., S. Merlin Gilbert Raj, and P. K. Mathew, "Performance analysis of U-slot and Y-slot patch antenna for wireless applications," *2014 International Conference on Electronics and Communication Systems (ICECS)*, 1–4, February 2014.
17. Naik, K. K. and P. A. V. Sri, "Design of hexadecagon circular patch antenna with DGS at Ku band for satellite communications," *Progress In Electromagnetics Research M*, Vol. 63, 163–173, 2018.
18. Mohamed, A. E., M. S. Sharawi, and A. Muqaibel, "Implanted dual-band circular antenna for biomedical applications," *Microwave and Optical Technology Letters*, Vol. 60, No. 5, 1125–1132, 2018.
19. Garg, R., P. Bhartia, I. Bahl, and A. Ittipiboon, *Micrstrip Antenna Design Hand Book*, Artech House, Norwood, MA, USA, 2001.